1,5,6,7-Tetrahydro-4H-indazol-4-ones as human neutrophil elastase (HNE) inhibitors

HHS Public Access

Author manuscript

Bioorg Med Chem Lett. Author manuscript; available in PMC 2022 November 15.

Published in final edited form as:

Bioorg Med Chem Lett. 2021 November 15; 52: 128380. doi:10.1016/j.bmcl.2021.128380.

1,5,6,7-Tetrahydro-4*H*-indazol-4-ones as human neutrophil elastase (HNE) inhibitors

Niccolo Cantini[a], **Letizia Crocetti**[a,*], **Gabriella Guerrini**[a], **Claudia Vergelli**[a], **Igor A. Schepetkin**[b], **Marco Pallecchi**[a], **Gianluca Bartolucci**[a], **Mark T. Quinn**[b], **Elisabetta Teodori**[a], **Maria Paola Giovannoni**[a]

[a]NEUROFARBA, Pharmaceutical and Nutraceutical Section, University of Florence, Via Ugo Schiff 6, 50019 Sesto Fiorentino, Italy

[b]Department of Microbiology and Cell Biology, Montana State University, Bozeman, MT 59717, USA

Abstract

Human neutrophil elastase (HNE) is a serine protease that is expressed in polymorphonuclear neutrophils. It has been recognized as an important therapeutic target for treating inflammatory diseases, especially related to the respiratory system, but also for various types of cancer. Thus, compounds able to inhibit HNE are of great interest in medicinal chemistry. In the present paper, we report the synthesis and biological evaluation of a new series of HNE inhibitors with an innovative 1,5,6,7-tetrahydro-4H-indazol-4-one core that was developed as a molecular modification of our previously reported indazole-based HNE inhibitors. Since the 1,5,6,7-tetrahydro-4*H*-indazol-4-one scaffold can occur in two possible tautomeric forms, the acylation/alkylation reactions resulted in a mixture of the two isomers, often widely unbalanced in favor of one form. Using analytical techniques and NMR spectroscopy, we characterized and separated the isomer pairs and confirmed the compounds used in biological testing. Analysis of the compounds for HNE inhibitory activity showed that they were potent inhibitors, with K_i values in the low nanomolar range (6–35 nM). They also had reasonable stability in aqueous buffer, with half-lives over 1 h. Overall, our results indicate that the 1,5,6,7-tetrahydro-4H-indazol-4-one core is suitable for the synthesis of potent HNE inhibitors that could be useful in the development of new therapeutics for treating diseases involving excessive HNE activity.

Keywords

Human neutrophil elastase; Inhibitors; 1,5,6,7-Tetrahydro-4H-indazol-4-ones; Isomers

*Corresponding author at: Dept. NEUROFARBA, Via Ugo Schiff 6, Sesto Fiorentino 50019, Firenze, Italy. letizia.crocetti@unifi.it (L. Crocetti).

Declaration of Competing Interest

The authors declare that they have no known competing financial interests or personal relationships that could have appeared to influence the work reported in this paper.

Appendix A. Supplementary data

Supplementary data to this article can be found online at https://doi.org/10.1016/j.bmcl.2021.128380.

Human neutrophil elastase (HNE) is a serine protease that is normally expressed in polymorphonuclear neutrophils (PMNs).[1] It plays an important role in many physiopathological processes, such as antimicrobial defense, inflammation, maintenance of tissue homeostasis, and it has been recognized as an important target for treating inflammatory diseases, especially related to the respiratory system.[2,3] HNE is released into the extracellular space following neutrophil degranulation or neutrophil extracellular trap (NET) formation in a process known as NETosis.[4] Neutrophils make up approximately 40–60 percent of the white blood cells in our bodies, and they are the first line of defense against invading pathogens where they participate in development of the inflammatory cascade.[5] Neutrophils appear to possess both pro- and antitumor properties,[6,7] and recent studies indicate that there are two neutrophil phenotypes N1 and N2, antitumor and pro-tumorigenic neutrophils, respectively.[8] The Tumor-Associated Neutrophils (TANs) can promote the onset of tumor growth by releasing of reactive oxygen and nitrogen species (ROS and RSN) or proteases.[9] This is not surprising, given the close resemblance between neutrophils and cancer cells.[10] Recently, some evidence suggest that NETs are also involved in the tumor microenvironment.[11,12] Specifically, HNE expression and activity seem to be up regulated and implicated in primary tumor onset, growth, and metastasis of breast, lung, prostate, and colon cancers.[13,14] In lung cancer patients, elevated serological HNE positively correlates not only with disease severity but also with progression of the disease itself. Moreover, enhanced HNE activity can also be detected indirectly through accumulation of a specific degradation product of elastin, called EL-NE,[15] suggesting that cancer is a potent inducer of neutrophil elastase. Several mechanisms have been proposed for the tumorigenic activity of HNE. First, HNE can directly stimulate proliferative pathways via membrane receptors, such as epidermal growth factor receptor (EGFR) and toll-like receptor 4 (TRL4), inducing mitogen activated protein kinase (MAPK) signalling. For example, in breast and prostate cancer cells, HNE acts through MAPK to induce ERK phosphorylation.[13] HNE released from neutrophils may also contribute to tumorigenesis by inactivating tumor suppressors and inducing angiogenesis.[14] The formation of NETs has also been implicated in the process of carcinogenesis, favouring the metastatic cascade. In addition, the tumor cells themselves are able to release proteases, which is a very important event in metastasis that allows the tumor to degrade some physiological barriers consisting of elastin (connective tissue), collagen, and proteoglycans (cartilage), finally facilitating progression of the disease.[16] Based on this information, it is clear that HNE could be of great interest both as a diagnostic marker and a therapeutic target for some types of cancer.

We have been studying HNE inhibitors extensively, investigating a variety of structures, either bicyclic or monocyclic, and our efforts enabled us to discover many potent compounds with IC_{50} values in the nanomolar range.[17–21] Recently, Boehringer Ingelheim GmbH developed a series of new HNE inhibitors whose scaffold consists of a pyrimidine fused with a cyclopentanone or cyclohexanone nucleous.[22,23] Based on this approach and following a similar strategy, we obtained molecular hybrids by replacing the phenyl ring of the indazole (the most promising and interesting scaffold of our previous series)[24] with a cyclohexanone nucleus present in the molecules patented by Boehringer Ingelheim. Therefore, in the present paper, we report the synthesis and biological evaluation as HNE inhibitors of a new series of compounds containing an innovative 1,5,6,7-tetrahydro-4H-

indazol-4-one core that is substituted at positions 1 and 5 with those groups that have given the best results in our previous series of the indazole-based HNE inhibitors[24] (Fig. 1).

The 1,5,6,7-tetrahydro-4*H*-indazol-4-one scaffold can occur in two possible tautomeric forms, as reported in the literature.[25]

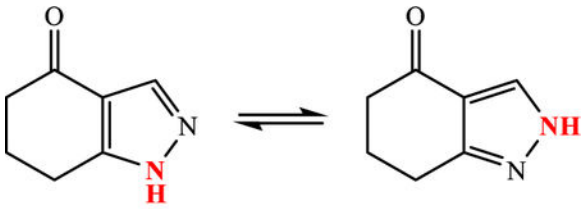

N1-H **N2-H**

For this scaffold, the N1 form is reported as the most abundant; however, the percentage of the two tautomers in solution depends on the type of solvent, solvent polarity, reaction medium and type of reactive used.[25] During alkylation and acylation reactions, it was possible to observe a mixture of the two isomers, often widely unbalanced in favor of one form. Thus, we performed an in-depth study of this issue, including the use of different techniques (analytic approaches and NMR spectroscopy) for the characterization and separation of the isomer pairs obtained.

The synthetic procedures for obtaining the final products are described in Schemes 1–3. Scheme 1 shows the synthesis of the reagent **2** (panel **A**) and of the final compounds **6a-h** and **7a-g** (panel **B**). The intermediate **1**[26] was transformed into the corresponding iodinated reagent **2** with sodium iodide in acetone at room temperature (panel **A**). In panel **B,** the commercial 1,3-cyclohexandione **3** was treated with DMF-DMA at reflux affording the 2-[(dimethylamino)methylene]cyclo-hexane-1,3-dione **4**,[25] which was then cyclized with hydrazine to the key intermediate **5**.[25] As expected, the acylation reaction performed with m-toluoyl chloride or cyclopropanecarbonyl chloride in dichloromethane and triethylamine resulted in a mixture of isomers (**6a**/**7a** and **6b**/**7b**, respectively). It is possible to achieve the same trend in alkylation reactions by performing reactions under standard conditions and using various reagents (**6d**/**7d**, **6e**[27]/**7e**[27], **6f**/**7f** and **6g**/**7g**) as well as in coupling reactions with 3-(trifluoromethyl)phenylboronic acid, copper (II) acetate and triethylamine in dichloromethane (**6c**/**7c**[28]). The Boc removal on derivative **6g** with dichloromethane and trifluoroacetic acid led to the final compound **6h**.

To understand the course of the reactions and in particular which isomer is obtained in greater amounts, an in-depth NMR spectroscopy study was performed to assign the correct structure to both isomers. The ^{1}H NMR spectra of the two isomers formed in the reaction were very similar to each other and did not allow a distinction, differing only for the 3-CH pyrazole chemical shift, which was more pronounced for the acyl derivatives (about 0.7 ppm), lower for the coupling derivatives **6c/7c** (0.3 ppm), and very slight for the alkyl derivatives (about 0.1 ppm). The use of 2D-NMR techniques, including Heteronuclear Single Quantum Correlation (HSQC) and Heteronuclear Multiple Bond Correlation (HMBC), provided complementary information and allowed us to establish the

exact structure of the isomers (see spectra in Supporting Information). In particular, we observed the presence of the coupling between the pyrazole 3-CH and the CH_2 (for alkyl derivatives) or the carbonyl carbon (for acyl derivatives) that is possible only in the N2 isomers, while it was absent in the N1 isomers. The results obtained are not completely in agreement with the data reported by Claramunt et al.,[25] since the N1-isomer prevailed only in the cyclopropanecarbonyl derivatives **6b/7b** (ratio N2/N1 about 1:4), while the N2-isomer was always the most abundant for all other compounds (ratio N2/N1 3:1).

Scheme 2 shows the synthesis of the 5-mono and 5,5-dibromo derivatives of type **9** and **10**. The key intermediate **5**[25] was treated with trimethylphenylammonium tribromide to obtain a mixture of the mono-bromo (**8a**[29]) and di-bromo (**8b**) derivatives, which were separated by flash chromatography. Acylation or alkylation of intermediates **8a,b** with the appropriate reagent under the same conditions reported above resulted a mixture of N1/N2 isomers **9** and **10**, with the only exception being compounds **9c** and **9d**, for which only the N2 isomer was obtained. As for compounds **6** and **7**, structure assignment for compounds **9** and **10** was performed with the aid of bidimensional NMR spectroscopy (see spectra in Supporting Information). Furthermore, the 5-bromo-1,5,6,7-tetrahydro-4H-indazol-4-one (**8a**) was also modified by replacing the bromine atom with an *N*-methylpiperazine group to obtain compound **11**, which was unstable and unfortunately not suitable for further

Finally, Scheme 3 shows the synthesis of **14a-c** containing an amide function at position 4 of the tetrahydro-4H-indazol-4-one. The starting compound **4**[25] was cyclized to 1-phenyl-pyrazolocyclohexanone **12**,[27] which was subjected to reductive amination with ammonium acetate and sodium cyanoborohydride, resulting in the 4-aminoderivative **13**.[30] The final compounds **14a,b** were obtained by reacting intermediate **13** under the classic conditions with cyclopropanecarbonyl chloride and triethylamine in anhydrous dichloromethane. Compound **14c** was obtained by adding compound **13** and triethylamine to 3-methylbenzoyl chloride that was prepared *in situ* with triphenylphosphine and trichloroacetonitrile in anhydrous dichloromethane at room temperature.

To further unambiguously confirm the data obtained from the mono and bi-dimensional NMR spectra, a pair of *N*-benzylated **6d**/**7d** and *N*-acylated **6a/7a** isomers were analyzed using the GC–MS technique. Through Gas Chromatography (GC) coupled to a single quadrupole mass spectrometer (MS) with electronic ionization (EI), the sample was subjected to an interaction with high energetic electron (70 eV) that causes large fluctuations in the electric field around the neutral molecules and induces their ionization and fragmentation. Therefore, using this approach, it was possible to acquire the chromatogram and respective fragmentation spectra of isomers pairs. The retention times between **6d/7d** and **6a/7a**, respectively (Fig. S1 for **6d/7d** as example, supporting information), were not sufficiently different to be considered discriminatory. However, each chromatographic peak of **6d/7d** showed a mass spectrum that was different between the two isomers, and this allowed us to confirm their structures. Analysis of the MS spectra of **6d/7d** (Fig. S2, supporting information) showed that isomer (**7d**) had a principal peak at 294 *m*/*z* corresponding to the radical molecular ion, while the other isomer (**6d**) had more abundant fragments within that range, including 294 *m*/*z* itself, but the most intense signal was

at 293 *m*/*z*. Assuming that the latter is the N2-benzylated form, it may be hypothesized that the signal at 293 *m*/*z* is due to the formation of a very stable fragmented ion that is the result of the radical proton leaving from position 3 of the pyrazole, resulting in the re-arrangement shown in Fig. 2. In contrast, this rearrangement mechanism is less favored on N1-benzylated (**7d**). As a result of this difference, we proposed that the fragment at 293 *m*/*z* is in competition with the 135 *m*/*z* ion formation, which is likely to represent the nucleus without the m-CF_3-phenyl moiety. On the other hand, **7d**, which does not possess this stable intermediate, has a very intense peak at 135 *m*/*z*. The two isomers share in common the peak at 159 *m*/*z* corresponding to the 3-CF_3-tropylium cation. Thus, we conclude that the isomer forming the stable intermediate (**6d**) has the benzyl moiety linked to nitrogen at position 2 (N2), while **7d** is the corresponding N1 isomer. Unfortunately, isomers **6a**/**7a** had very similar MS-spectra. Therefore, it was not possible to distinguish between these *N*-acylated isomers (Fig. S3, supporting information).

The biological results of all new synthesized compounds are shown in Tables 1 and 2 and were compared with the reference drug Sivelestat. The data reported in Table 1 clearly show the importance of the *N*-CO group for HNE inhibitory activity and in particular when the CO group is linked to a nitrogen of the pyrazole. In fact, the only potent compounds were N2-or N1-acylated derivatives (**6a,b** and **7a,b** respectively), which had K_i values of 11–35 nM and were in the same range as the reference compound Sivelestat. The importance of the *N*-CO link involving the pyrazole nitrogen is in agreement with our previous results[20,24] and was further confirmed by the complete inactivity of *N*-benzyl derivatives **6d**/**7d** and **6e**/**7e** and of N-(m-CF_3-phenyl) derivatives **6c**/**7c** lacking the amide group. The movement of the amide on the fragment containing the piperazine also led to completely inactive compounds, with the only exception being isomers **6f**/**7f** which, however, were weak inhibitors (K_i = 16.6 μM for **6f** and 13 μM for **7f**). Similarly, compounds **14a-c** containing the amide function shifted to position 4 of the cyclohexanone were completely inactive.

Further assessment of the most potent compounds in this series indicated that there was no difference in activity between the two isomers of the cyclopropylcarbonyl derivatives (**6b**/**7b**), whereas the N2 isomer was about three-fold more potent than the N1 derivative for the m-toluoyl derivatives **6a**/**7a** (K_i = 11 nM for **6a** and 35 nM for **7a**).

The introduction of one or two bromines at position 5 of the core led to the potent HNE inhibitors **9a-d** and **10a,b**, with K_i = 6–18 nM (Table 2). Comparing these compounds with the corresponding 5-unsubstituted compounds **6a**, **6b** and **7b** (Table 1), we found that the introduction of one or two bromine atoms led to a general improvement in activity (i.e. 5-unsubstituted **6b** K_i = 25 nM versus 5-monobromo **9a** and 5,5-dibromo **9b**, K_i = 17 and 11 nM, respectively). On the other hand, there was no significant difference in activity between the mono- and di-bromo derivatives, as demonstrated by the couples **9a**/**9b**, **9c**/**9d** and **10a**/**10b**. The most potent HNE compounds were the m-toluoyl derivatives **9c** (K_i = 6 nM) and **9d** (K_i = 6 nM), which were about four times more active than the reference compound Sivelestat. As the 5-unsubstituted derivatives reported in Table 1, the removal of the amide group resulted in compounds low active or devoid of HNE inhibitory activity (compounds **9e, 9f, 10c** and **10d**).

To better understand the mechanism of action of the 1,5,6,7-tetrahydro-4H-indazol-4-one derivatives, we performed kinetic experiments with the active compounds. As shown in Figure 3, the representative double-reciprocal Lineweaver–Burk plots of fluorogenic substrate hydrolysis by HNE in the absence and presence of the compounds **6b** and **7a** indicate that these derivatives are indeed competitive HNE inhibitors. Similar results were observed with kinetic analysis of the other active derivatives (data not shown).

The stability in aqueous buffer for some compounds (**7a**, **9a**, **9b**, **10a**, **10b**) was also evaluated, and the results are reported in Table 3. The most stable compound was **9b** (5,5-dibromo-2-(cyclopropanecarbonyl)-2,5,6,7-tetrahydro-4H-indazol-4-one), which had $t_{1/2}$ = 4 h. Comparing the half-life of the mono-bromo **9a**/**10a** with the di-bromo derivatives **9b**/**10b**, we can hypothesize that the increased lipophilicity due to the additional bromine enhanced the time required for hydrolysis. In addition, comparison of the isomer pairs **9a**/**10a** ($t_{1/2}$ = 114.74 and 53.88 min, respectively) and **9b**/**10b** ($t_{1/2}$ = 234.84 and 57.06 min, respectively) confirmed that the N1-acylated compounds were more susceptible to hydrolysis than the corresponding N2 derivatives.

In addition, two pairs of isomers (**6a**/**7a** and **6d**/**7d**, *N*-acylated and *N*-alkylated derivatives, respectively) were selected to investigate their chemical stability over time towards the hydrolytic enzymes in human plasma samples. The samples were analyzed by LC-MS/MS operating in a multiple reaction monitoring (MRM) mode. The solution of each compound was verified by monitoring the variation of analyte concentration at different incubation times in human plasma samples. Each set of samples was incubated at 37 °C in triplicate using four different times (0, 30, 60, and 120 min) and pooled human plasma collected from healthy volunteers.[31] The analyte concentration (2.5 μM) used during the stability tests was generally lower than the corresponding Michaelis–Menten constant (K_M). Therefore, the enzymatic degradation rate is described by first-order kinetics. By plotting the natural logarithm of the quantitative data versus the incubation time, a linear function can be used, and its slope represents the degradation rate constant (k). The half-life ($t_{1/2}$) of each tested compound can be calculated as follows:

$$t_{1/2} = ln(1.25\,\mu M)/k$$

The results show that the isomer pair **6d/7d** maintained their spiked concentration for all of the incubation times, whereas the isomers **6a/7a** displayed a rapid degradation rate with an estimation half time of 6 min for both (see Figs. S4–S7 in Supporting Information).

In conclusion, the results obtained indicate that the 1,5,6,7-tetrahy-dro-4H-indazol-4-one core is suitable for the synthesis of HNE inhibitors. Many of the new compounds had K_i values in the nanomolar range, with **9c** and **9d** being the most potent compounds (Ki = 6 nM) and on the more interesting compounds it will be necessary to evaluate the selectivity against other proteases such as Chymotrypsin, Urokinase, Trypsin and Thrombin to plan their eventual development.

Of great importance were the spectroscopic and GC–MS studies, which allowed us to assign the correct structures to the N1 and N2 isomer pairs. In terms of inhibitory activity, the

two isomers N1 and N2 were very similar, with comparable potency. Regarding stability in aqueous buffer, which was satisfactory for most compounds ($t_{1/2}$ > 1 h), the N2 isomers were more stable than the corresponding N1 isomers. On the other hand, the rapid degradation rate of the active compounds **6a/7a** in human plasma, suggest the need to make targeted changes to increase stability or, for a possible development, to think about a different route of administration than the systemic one. Overall, our results indicate that the 1,5,6,7-tetrahydro-4H-indazol-4-one core is suitable for the synthesis of potent HNE inhibitors that could be useful in the development of new therapeutics for treating diseases involving excessive HNE activity.

Supplementary Material

Refer to Web version on PubMed Central for supplementary material.

Acknowledgments

This research was supported in part by National Institutes of Health IDeA Program Grants GM115371 and GM103474; USDA National Institute of Food and Agriculture Hatch project 1009546; and the Montana State University Agricultural Experiment Station.

References

1. Crocetti L, Quinn MT, Schepetkin IA, Giovannoni MP. A patenting perspective on human neutrophil elastase (HNE) inhibitors (2014–2018) and their therapeutic applications. Expert Opin Ther Pat. 2019;29:555–578. 10.1080/13543776.2019.1630379. [PubMed: 31204543]
2. Korkmaz B, Moreau T, Gauthier F. Neutrophil elastase, proteinase 3 and cathepsin G: Physicochemical properties, activity and physiopathological functions. Biochimie. 2008;90:227–242. 10.1016/j.biochi.2007.10.009. [PubMed: 18021746]
3. Von Nussbaum F, Li VMJ. Neutrophil elastase inhibitors for the treatment of (cardio) pulmonary diseases: into clinical testing with pre-adaptive pharmacophores. Bioorg Med Chem. 2015;25:4370–4381. 10.1016/j.bmcl.2015.08.049.
4. Papayannopoulos V, Metzler KD, Hakkim A, Zychlinsky A. Neutrophil elastase and myeloperoxidase regulate the formation of neutrophil extracellular traps. J Cell Biol. 2010;191:677–691. 10.1083/jcb.201006052. [PubMed: 20974816]
5. Pham CTN. Neutrophil serine proteases: specific regulators of inflammation. Nat Rev Immunol. 2006;6:541–550. 10.1038/nri1841. [PubMed: 16799473]
6. Shaul ME, Fridlender ZG. Neutrophils as active regulators of the immune system in the tumor microenvironment. J Leukoc Biol. 2017;102:343–349. 10.1189/jlb.5MR1216-508R. [PubMed: 28264904]
7. Wu L, Saxena S, Awaji M, Singh RK. Tumor-associated neutrophils in cancer: going pro. Cancers. 2019;11:P5641–20. 10.3390/cancers11040564.
8. Fridlender ZG, Albelda SM. Tumor-associated neutrophils: friend or foe? Carcinogenesis. 2012;33:949–955. 10.1093/carcin/bgs123. [PubMed: 22425643]
9. Antonio N, Bonnelykke-Behrndtz ML, Ward LC, et al. The wound inflammatory response exacerbates growth of pre-neoplastic cells and progression to cancer. EMBO J. 2015;34:2219–2236. 10.15252/embj.201490147. [PubMed: 26136213]
10. Sato T, Takahashi S, Mizumoto T, et al. Neutrophil elastase and cancer. Surg Oncol. 2006;15:217–222. 10.1016/j.suronc.2007.01.003. [PubMed: 17320378]
11. Huang H, Zhang H, Onuma AE, Tsung A. Neutrophil elastase and neutrophil extracellular traps in the tumor microenvironment. Birbrair A (ed.), Tumor Microenvironment, Advances in Experimental Medicine and Biology 1263, Springer; 2020. 10.1007/978-3-030-44518-8_2.

12. Masucci MT, Minopoli M, Del Vecchio S, Carriero MV. The emerging role of neutrophil extracellular traps (NETs) in tumor progression and metastasis. Front Immunol. 2020;11:1749. 10.3389/fimmu.2020.01749. [PubMed: 33042107]
13. Lerman I, Hammes SR. Neutrophil elastase in the tumor microenvironment. Steroids. 2018;133:96–101. [PubMed: 29155217]
14. Lerman I, Garcia-Hernandez ML, Rangel-Moreno J, et al. Infiltrating myeloid cells exert protumorigenic actions via neutrophil elastase. Mol Cancer Res. 2017;15: 1138–1152. 10.1158/1541-7786.MCR-17-0003. [PubMed: 28512253]
15. Kristensen JH, Karsdal MA, Sand JMB, et al. Serological assessment of neutrophil elastase activity on elastin during lung ECM remodelling. BMC Pulm Med. 2015;15: 53. 10.1186/s12890-015-0048-5. [PubMed: 25935650]
16. Lu P, Weaver VM, Werb Z. The extracellular matrix: a dynamic niche in cancer progression. J Cell Biol. 2012;196:395–406. 10.1083/jcb.201102147. [PubMed: 22351925]
17. Crocetti L, Giovannoni MP, Cantini N, et al. Novel sulfonamide analogs of sivelestat as potent human neutrophil elastase inhibitor. Front Chem. 2020;8:795. 10.3389/fchem.2020.00795. [PubMed: 33033716]
18. Cantini N, Khlebnikov AI, Crocetti L, et al. Exploration of nitrogen heterocycle scaffolds for the development of potent human neutrophil elastase inhibitors. Bioorg Med Chem. 2021;29, 115836. 10.1016/j.bmc.2020.115836. [PubMed: 33218895]
19. Giovannoni MP, Crocetti L, Cantini N, et al. New 3-unsubstituted isoxazolones as potent human neutrophil elastase inhibitors: synthesis and molecular dynamic simulation. Drug Dev Res. 2020;81:338–349. 10.1002/ddr.21625. [PubMed: 31800122]
20. Crocetti L, Giovannoni MP, Schepetkin IA, et al. 1H-pyrrolo[2,3-b]pyridine: A new scaffold for human neutrophil elastase (HNE) inhibitors. Bioorg Med Chem. 2018;26: 5583–5595. 10.1016/j.bmc.2018.09.034. [PubMed: 30385225]
21. Giovannoni MP, Schepetkin IA, Quinn MT, et al. Synthesis, biological evaluation, and molecular modelling studies of potent human neutrophil elastase (HNE) inhibitors. J Enzyme Inhib Med Chem. 2018;33:1108–1124. 10.1080/14756366.2018.1480615. [PubMed: 29969929]
22. Peters S, Anderskewitz R, Gnamm C, et al. Substituted bicyclic dihydropyrimidones and their use as inhibitors of neutrophil elastase activity. US 9458113 B2. 2016.
23. Gnamm C, Oost T, Peters S, et al. Substituted bicyclic dihydropyrimidones and their use as inhibitors of neutrophil elastase activity. US 9670166 B2. 2017.
24. Crocetti L, Schepetkin IA, Cilibrizzi A, et al. Optimization of N-benzoylindazole derivatives as inhibitors of human neutrophil elastase. J Med Chem. 2013;56: 6259–6272. 10.1021/jm400742j. [PubMed: 23844670]
25. Claramunt RM, López C, Pérez-Medina C, Pinilla E, Torres MR, Elguero J. Synthesis and structural study of tetrahydroindazolones. Tetrahedron. 2006;62:11704–11713. 10.1016/j.tet.2006.09.043.
26. Sharma RK, Younis Y, Mugumbate G, et al. Synthesis and structure–activity-relationship studies of thiazolidinediones as antiplasmodial inhibitors of the Plasmodium falciparum cysteine protease falcipain-2. Eur J Med Chem. 2015;90: 507–518. 10.1016/j.ejmech.2014.11.061. [PubMed: 25486422]
27. Spanò V, Parrino B, Carbone A, et al. Pyrazolo[3,4-h]quinolines promising photosensitizing agents in the treatment of cancer. Eur J Med Chem. 2015;102: 334–351. 10.1016/j.ejmech.2015.08.003. [PubMed: 26295175]
28. Guo S, Song Y, Huang Q, et al. Identification, synthesis, and pharmacological evaluation of tetrahydroindazole based ligands as novel antituberculosis agents. J Med Chem. 2010;53:649–659. 10.1021/jm901235p. [PubMed: 20000470]
29. Bolea C, Celanire S. Substituted 5,6-dihydro-4h-thiazolo[4,5-e]indazoles and their use as positive allosteric modulators of metabotropic glutamate receptors. U.S. Pat. Appl. Publ US8697744B2, 2014.
30. Lain S, Drummond C, Van Leeuwen I, Haraldsson M, et al. Tetrahydroindazoles for use in the treatment of cancer and viral infections and their preparation. PCT Int. Appl WO2017077280A1, 2017.

31. Menicatti M, Pallecchi M, Bua S, et al. Resolution of co-eluting isomers of anti-inflammatory drugs conjugated to carbonic anhydrase inhibitors from plasma in liquid chromatography by energy-resolved tandem mass spectrometry. J Enzyme Inhib Med Chem. 2018;33:671–679. 10.1080/14756366.2018.1445737. [PubMed: 29536775]

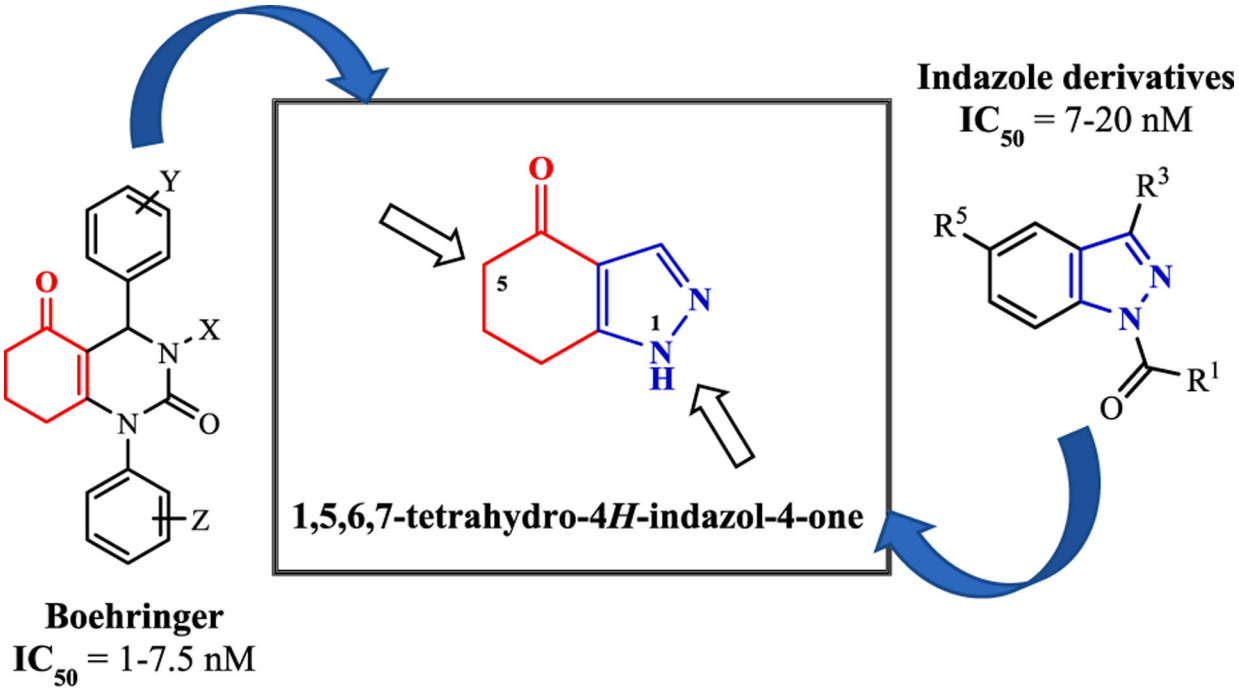

Fig. 1.
Design of new 1,5,6,7-tetrahydro-4*H*-indazol-4-ones.

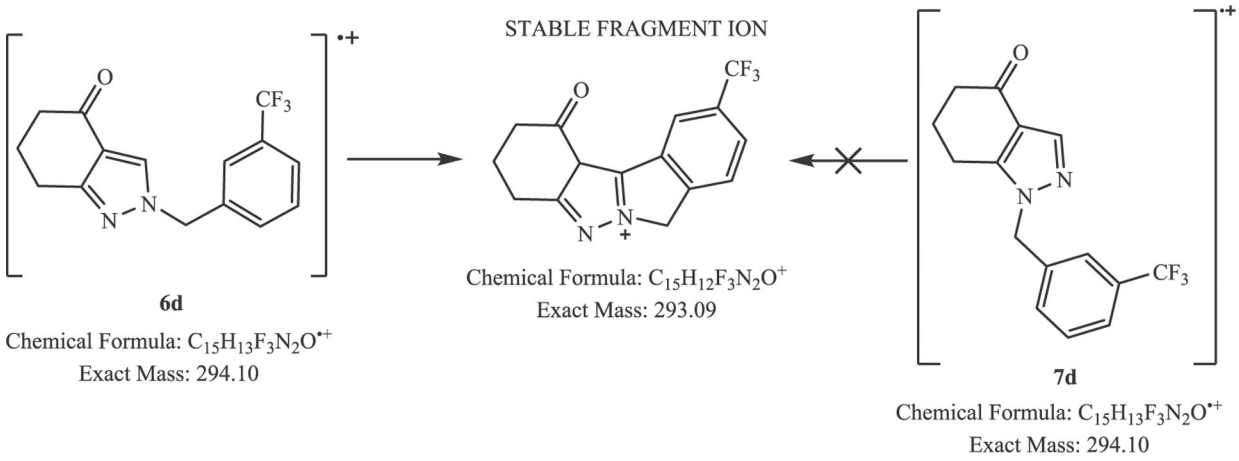

Fig. 2.
Different rearrangement of isomers **6d/7d**.

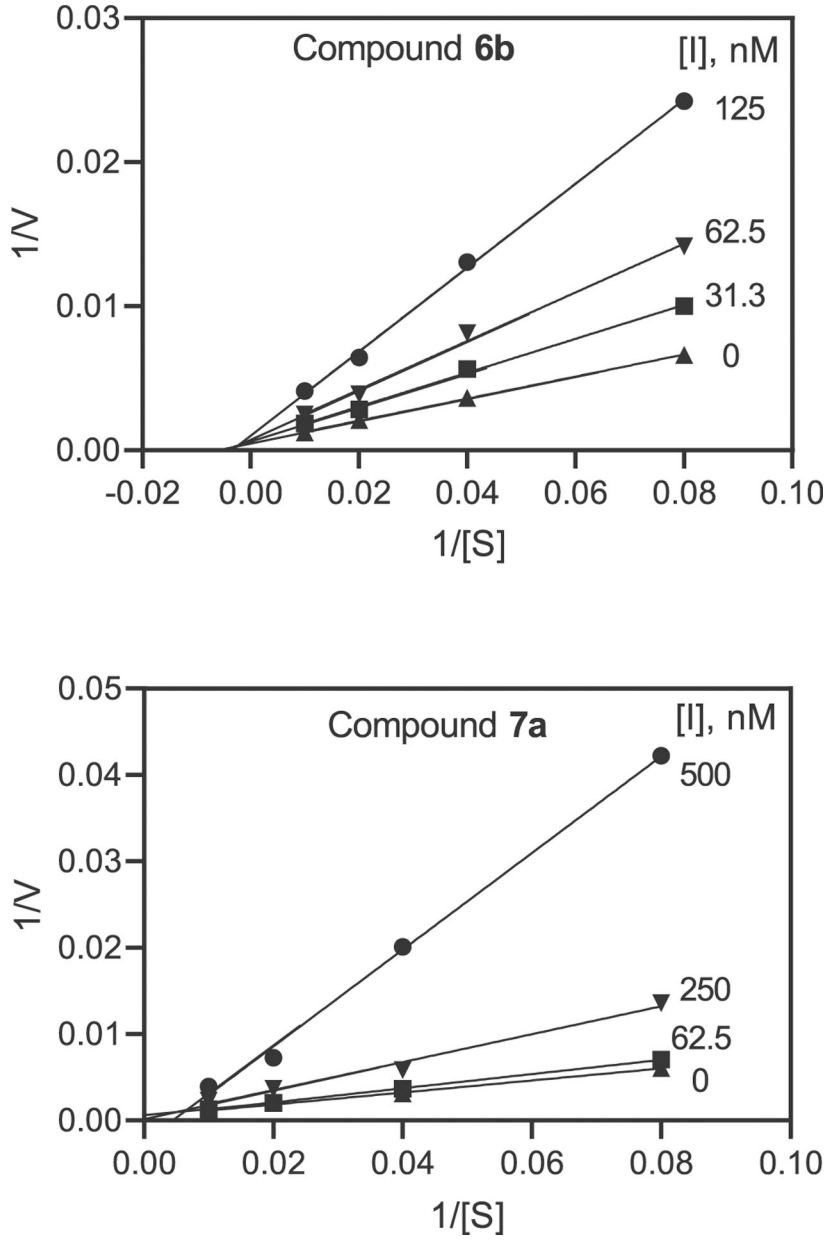

Fig. 3.

Kinetics of HNE inhibition by selected derivatives. Representative double-reciprocal Lineweaver-Burk plots are shown. Representative plots are from two independent experiments.

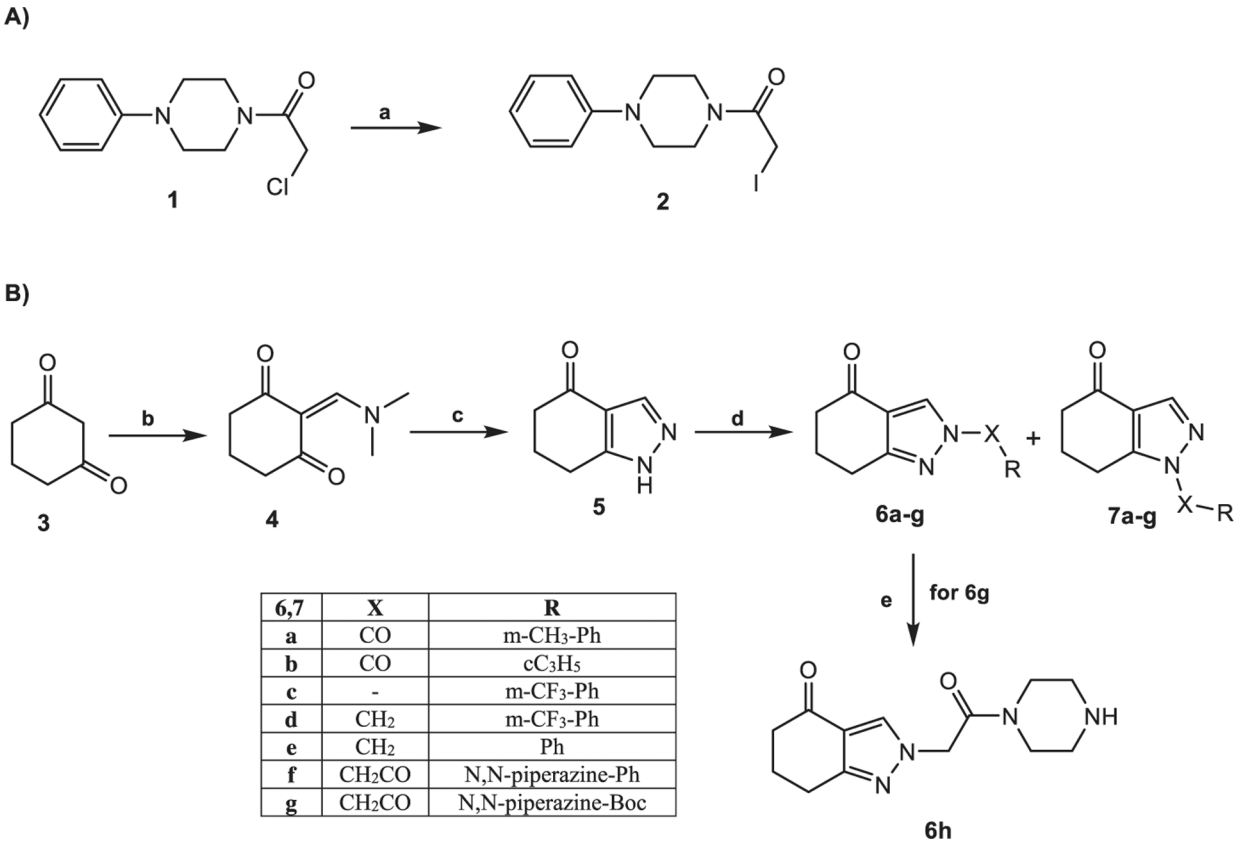

6,7	X	R
a	CO	m-CH_3-Ph
b	CO	cC_3H_5
c	-	m-CF_3-Ph
d	CH_2	m-CF_3-Ph
e	CH_2	Ph
f	CH_2CO	N,N-piperazine-Ph
g	CH_2CO	N,N-piperazine-Boc

Scheme 1.

[a]Reagents and conditions: a) Acetone, NaI, r.t., 16 h; b) DMF-DMA, reflux, 1 h; c) MeOH/H_2O, $NH_2NH_2{\cdot}H_2O$, NaOH, reflux, 2 h and then AcOH/H_2O, 110 °C, 1.5 h; d) for **6a,b** and **7a,b**: appropriate R-COCl, Et_3N, anhydrous CH_2Cl_2, 0 °C, 2 h and then r.t., 2 h; for **6c** and **7c**: $(CH_3COO)_2Cu$, dry CH_2Cl_2, 3-(trifluoromethyl)phenylboronic acid, Et_3N, r.t., 12 h; for **6d-g** and **7d-g**: CH_3CN anhydrous, appropriate alkylating agent, K_2CO_3, reflux, 3 h; **e)** CH_2Cl_2:CF_3COOH (6:1), 0 °C, then r.t., 2 h.

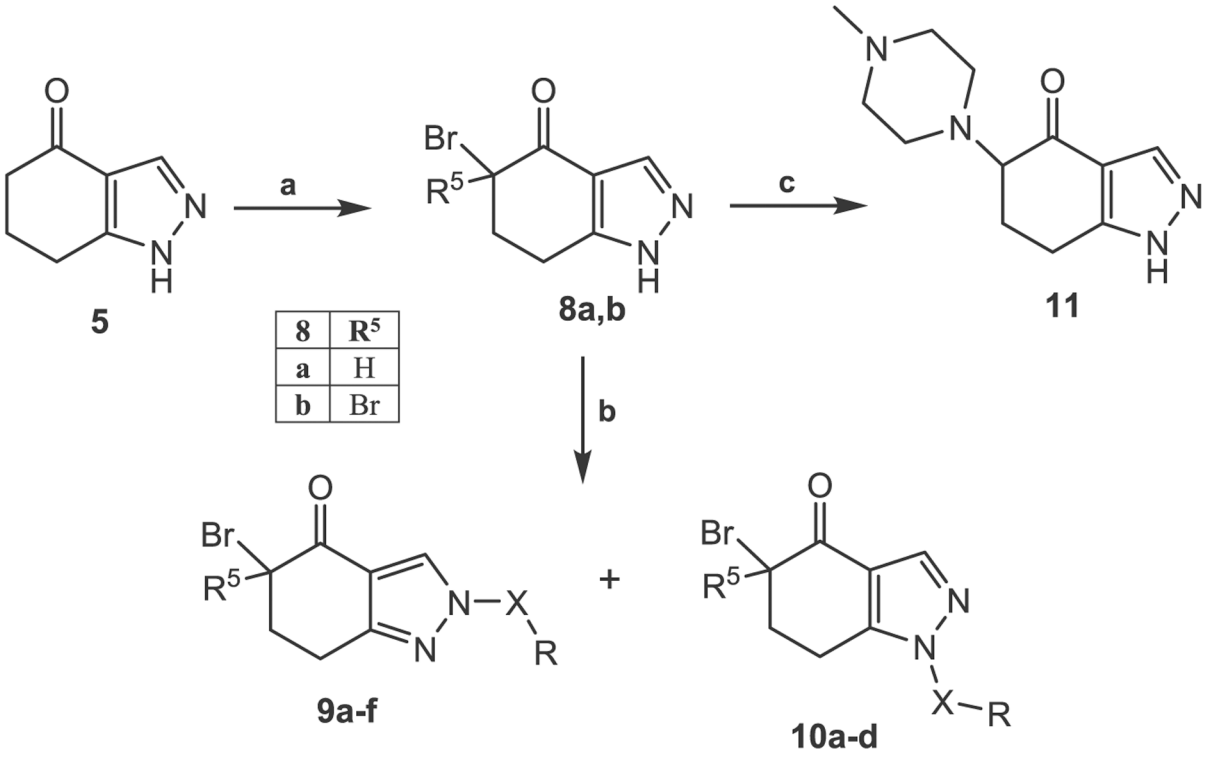

8	R^5
a	H
b	Br

9	X	R	R^5
a	CO	cC_3H_5	H
b	CO	cC_3H_5	Br
c	CO	m-CH_3-Ph	H
d	CO	m-CH_3-Ph	Br
e	CO	O-tBu	H
f	CH_2CO	N,N-piperazine-Ph	H

10	X	R	R^5
a	CO	cC_3H_5	H
b	CO	cC_3H_5	Br
c	CO	O-tBu	H
d	CH_2CO	N,N-piperazine-Ph	H

Scheme 2.

[a]Reagents and conditions: a) anhydrous CH_2Cl_2, $[PhNMe_3][Br]_3$, 100 °C, 3 h; b) for **9a-e** and **10a-c**: appropriate R-COCl, Et_3N, anhydrous CH_2Cl_2, 0 °C, 2 h and then r.t., 2 h; for **9f** and **10d**: anhydrous CH_3CN, compound **2**, K_2CO_3, reflux, 3 h; **c)** dry DMF, *N*-methylpyperazine, K_2CO_3, r.t., 24 h.

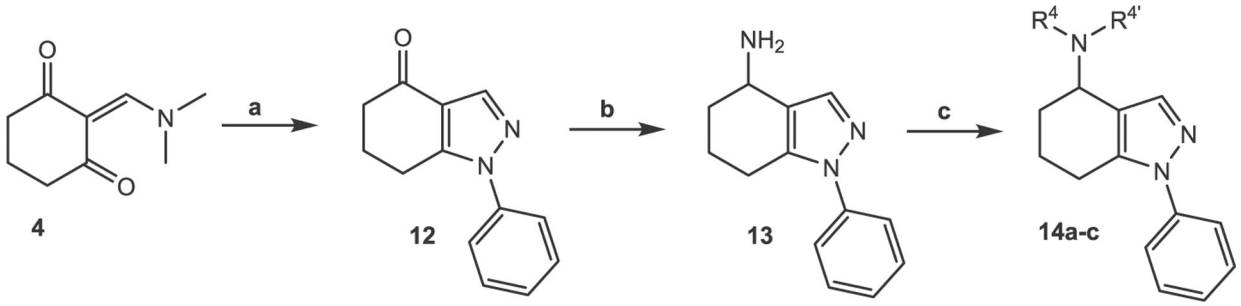

14	R^4	$R^{4'}$
a	CO-cC_3H_5	CO-cC_3H_5
b	H	CO-cC_3H_5
c	H	CO-m-CH_3-Ph

Scheme 3.

[a]Reagents and conditions: a) MeOH/H_2O, $PhNHNH_2$, NaOH, reflux, 2 h, then AcOH/H_2O, 110 °C, 1.5 h; b) i-PrOH, CH_3COONH_4, molecular sieves, $NaBH_3CN$, 70 °C, 24 h; c) for **14a,b:** dry CH_2Cl_2, cyclopropanecarbonyl chloride, Et_3N, 0 °C, 2 h and then r.t., 2 h; for **14c:** 3-methylbenzoic acid, CCl_3CN, dry CH_2Cl_2, PPh_3, r.t., 4 h and then Et_3N, r.t., 12 h.

Table 1

HNE inhibitory activity of compounds **6a-h**, **7a-g**, and **14a-c**.

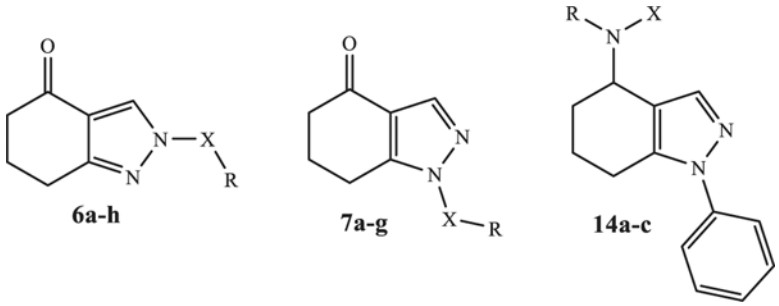

Compound	X	R	K_i (μM)[a]
6a	CO	m-CH_3-Ph	0.011 ± 0.03
6b	CO	cC_3H_5	0.025 ± 0.003
6c	–	m-CF_3-Ph	N.A.[b]
6d	CH_2	m-CF_3-Ph	N.A.[b]
6e	CH_2	Ph	N.A.[b]
6f	CH_2CO	*N,N*-piperazine-Ph	19.6 ± 2.4
6g	CH_2CO	*N,N*-piperazine-Boc	N.A.[b]
6h	CH_2CO	*N,N*-piperazine	N.A.[b]
7a	CO	m-CH_3-Ph	0.035 ± 0.011
7b	CO	cC_3H_5	0.025 ± 0.004
7c	–	m-CF_3-Ph	N.A.[b]
7d	CH_2	m-CF_3-Ph	N.A.[b]
7e	CH_2	Ph	N.A.[b]
7f	CH_2CO	*N,N*-piperazine-Ph	13.0 ± 2.1
7g	CH_2CO	*N,N*-piperazine-Boc	N.A.[b]
14a	CO-cC_3H_5	CO-cC_3H_5	N.A.[b]
14b	H	CO-cC_3H_5	N.A.[b]
14c	H	CO-m-CH_3-Ph	N.A.[b]
Sivelestat	–	–	0.024 ± 0.009

[a] Ki values are presented as the mean ± SD of three independent experiments.

[b] N.A.: no inhibitory activity was found at the highest concentration of compound tested (50 μM).

Table 2

HNE inhibitory activity of compounds **9a-f** and **10a-d**.

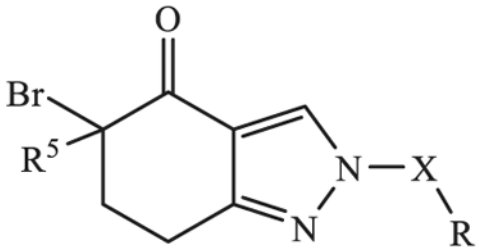

9a-f

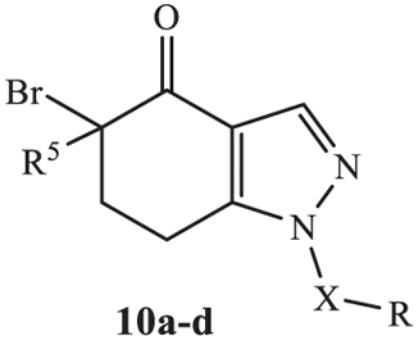

10a-d

Compounds	X	R^5	R	K_i (μM)[a]
9a	CO	H	cC_3H_5	0.017 ± 0.002
9b	CO	Br	cC_3H_5	0.011 ± 0.001
9c	CO	H	m-CH_3-Ph	0.006 ± 0.001
9d	CO	Br	m-CH_3-Ph	0.006 ± 0.001
9e	COO	H	tBu	N.A.[b]
9f	CH_2CO	H	*N,N*-piperazine-Ph	N.A.[b]
10a	CO	H	cC_3H_5	0.018 ± 0.004
10b	CO	Br	cC_3H_5	0.014 ± 0.003
10c	COO	H	tBu	0.29 ± 0.05
10d	CH_2CO	H	*N,N*-piperazine-Ph	N.A.[b]
Sivelestat				0.024 ± 0.009

[a] Ki values are presented as the mean ± SD of three independent experiments.

[b] N.A.: no inhibitory activity was found at the highest concentration of compounds tested (50 μM).

Table 3

Half-life ($t_{1/2}$) for the spontaneous hydrolysis of selected derivatives.

Compound	$t_{1/2}$ (min)
7a	98.1 ± 3.5
9a	114.74 ± 6.7
10a	38.7 ± 4.1
9b	234.84 ± 18.2
10b	57.1 ± 1.7